Jacobi-Fourier phase masks as ophthalmic elements to correct presbyopia.

A. Salas-Sanchez[1], E. González-Amador[1*], A. Padilla-Vivanco[1], C. Toxqui-Quitl[1], J. Arines[2,3], E. Acosta[2].

[1]*Universidad Politécnica de Tulancingo, Ingenierías No. 100, 43629, Tulancingo, Hidalgo, México.*
[2]*Universidade de Santiago de Compostela, Facultade de Óptica e Optometría, Dept. Física Aplicada, Santiago de Compostela, España.*
[3]*iMATUS(Instituto de Materiales) Universidade de Santiago de Compostela, Santiago de Compostela, España*
**Correspondence: Enrique González Amador.*
E-mail. enrique.gonzalezam@upt.edu.mx

Abstract

Purpose: Presbyopia correction involves studies such as lens design, clinical study, and the development of objective metrics, such as the visual Strehl ratio. We will analyze the potential use of the Jacobi-Fourier phase mask (JFPM) as an ophthalmic element for Presbyopia correction. This fact, to develop a contact or intraocular lens whose performance is nearly insensitive to changes in pupil diameter.

Methods: Numerical simulations based on Fourier Optics were made to evaluate three different Jacobi-Fourier polynomials of different radial order with the aim of providing a range of clear vision of one diopter. The performance was evaluated in three different pupil sizes (6, 4, 2) mm. Polychromatic images were simulated using three different wavelengths (656.3 nm, 587.6 nm and 486.1 nm). The Neural Transfer function was included in the simulation. We used the VScombined, as objective metric currently used in visual optics.

Results: The results show that Jacobi-Fourier Polynomials are suitable for designing optical solutions for presbyopia.

Conclusions: The use of Jacobi-Fourier phase masks as ophthalmic elements for presbyopia show promising results, with good range of clear vision, reduced pupil dependence and chromatic aberration.

Key Points

- The Jacobi Fourier Phase Masks as ophthalmic elements to correct presbyopia show less artifacts, reduced pupil dependence and chromatic aberration compared to the trefoil mask reported in literature.
- For the analysis of the results, a new metric has been introduced that combines the contribution of the phase element and the neuronal function to determine the method performance.
- The metrics show that the proposed method reachs its objective, and the threshold contrast function indicates that the images are clearly perceived by the human brain.

Keywords: pupil diameter; presbyopia; ophthalmic element; Neural Transfer Function; Jacobi-Fourier; visual Strehl.

1. Introduction

Presbyopia is the inability to observe objects at short distances that affect people mostly over 45 years of age, due to the natural loss of flexibility of the crystalline lens, making it impossible to focus on objects at short distances[1].

There are various solutions, such as contact lenses, progressive lenses, or intraocular surgery[2-5]. There is a type of contact lens or intraocular lens known as EDOF lens. There are other non-continuous solutions that provides extended depth of field as for example the one proposed by Mira-Agudelo[6] based on what is known as light sword lens. This solution behaves like an axicon providing a long focal spot that provides a good range of clear vision.

Most of EDOF commercial solutions are based on spherical aberration. There are also a few works proposing the use of alternative phases. There is a recent proposal made by Galinier et al. based on the spiralization of an astigmatic lens to extend the depth of focus[7]. Earlier there were other solutions initially proposed in the field of wavefront coding [8-11]. The first one to propose this use of kind phase masks was Cathey[8]. Later Almaguer et al.[12] suggest the use of a cubic phase mask of the kind $Ar^3\cos(3\theta)$, being the parameter A the peak to valey of the phase mask, and r and θ, the radial and angular coordinates. Recently González Amador et al. [13] proposes the use of a new base of polynomials, the Jacobi-Fourier polynomials, for building phase masks with application in wavefront coding. They found that: 1) JFP provided more flexibility to the design that the Zernike polynomials; 2) they reduce the amount of artifacts and thus, improves image quality[13,14].

Wavefront coding[15] (WFC) is an optical-digital technique based on the use of a phase mask that makes that the Optical Transfer Function (OTF) of the system is nearly independent of the object position in a range of distances, providing invariance to defocus. Due to its ability to generate a defocus-invariant OTF this elements can be a solution to presbyopia. The invariance is achieved at a cost to the sharpness of the image. In WFC the loss of sharpness can be overcome thanks to digital image processing. In the case of using WFC phase mask elements for correcting presbyopia, the postprocessing for image enhancement have to be made by the visual system. So, there are limitations on the shape of the phase masks. Visual system provides an image enhancement based on contrast enhancement provided by the Neural Transfer Function[16,17] (NTF), so it is important that the phase mask provides images similar to the object but with accepted reduction in contrast loss.

In this work we analyze the performance of JFP for extending the depth of focus and use them for building optical elements (contact or intraocular lenses) for correcting presbyopia. We will perform the comparison by numerical simulations based on Fourier Optics. We compared three JFP and spherical aberration, using polychromatic light and for different pupil sizes. We used the VScombined, objective metric currently used in visual optics[18-20]. We also show the images obtained in the simulation for clarity.

1.1 Jacobi Fourier Polynomials

The general definition of Jacobi Fourier polynomials can be found in reference 13. In this work we reduced the variability of options to the family of JFP with $p = 7,\ p = 8$, and $p = 9$ and the value of $m = 3$, reducing the general equation to:

$$S(\rho, \theta) = k\alpha\rho^{\frac{p-1}{2}}\cos(3\theta), \tag{1}$$

where, $\rho = \sqrt{x^2 + y^2}$; and $\theta = \tan^{-1}(y/x)$, k is the wave number, α is the strength of the mask, this parameter determines the difference in the optical path. The parameter p is an integer constant that describes the family to which each mask belongs. The phase induced by the optical element is modeled by:

$$\alpha = \Delta t(n(\lambda) - 1), \tag{2}$$

The thickness Δt of the phase mask is calculated from Eq. 2, considering the material and the dispersion for the three wavelengths. The method for the optimal value is described in section 3.

2. Numerical Evaluation

To evaluate the Jacobi-Fourier phase mask (JFPM), we used computational Fourier optics from which we were able to simulate the retinal image provided by different phase masks, and the different visual Strehl criteria. We used in the simulations the JFPM obtained from eq. 1 with $p = 7,\ p = 8,\ p = 9$. and different α, the strength of the JFPM.

We considered for the simulations the simplified model eye[21] with 16.6 mm focal length. We considered three different pupil diameters (2, 4 and 6) mm to check the pupil dependence of the phase masks. We took into account the chromatic dispersion using three wavelengths, ($\lambda_1 = 656.3\ nm$, $\lambda_2 = 587.6\ nm$ and $\lambda_3 = 486.1\ nm$). We defined a range of clear vision from 6 m to 1 m, so we repeated the simulations for these two distances. We included in the simulations the Stiles- Crawford (SC)[22] effect and the Neural Transfer Function (NTF). The NTF is calculated as the product of the EmG contrast sensitivity model[16] and the skew effect, it is described by the Eq. 3.

$$NTF = \left\{ e^{\left(-\frac{f}{f_0}\right)} - ae^{\left(-\left(\frac{f}{f_1}\right)^2\right)} \right\} \cdot \begin{Bmatrix} 1 - e^{\left(-\frac{(f-f_2)}{b}\right)} * sin^2(2\theta) & (f > 3.48) \\ 1 & (f \leq 3.48) \end{Bmatrix}, \tag{3}$$

where f is the spatial frequency, f_0 is the lowest frequency, f_1 is the highest frequency, and a is the attenuation factor at low frequencies, the parameters that best fit according to Whatson & Ahumada[15] are: $f_0 = 33.36\ cyc/deg$, $f_1 = 5.38\ cyc/deg$ and $a = 0.92$. On the other hand, b and f_2 are the parameters that describe the contrast attenuation, the optimal values are $b = 13.57\ cyc/deg$ and $f_2 = 3.48\ cyc/deg$. The *NTF* is included in the calculation of the *OTF* of the system ($OTF_{sys} = OTF * NTF$).

We used as optotype the "E" Snellen. We have considered a size 0.1 Log Mar optotype with a spatial frequency of around 23.3 cyc/deg located on a range of 6 m to 1 m. We also considered the chromatic aberration that occurs in the eye using the model proposed by Thibos[23] et al. The mathematical expression is given by

$$D(\lambda) = u - \frac{v}{\lambda - c}, \tag{4}$$

where $u = 1.68$, $v = 0.63$, and $c = 0.21$.

For a wavelength centered on λ_0, the blurring of other wavelengths is determined as:

$$D(\lambda, \lambda_0) = D(\lambda) - D(\lambda_0). \tag{5}$$

Finally, we used the Zernike polynomials for quantifying blur in micrometers for the diameter *d*.

$$c_2^0 = \frac{D(\lambda, \lambda_0)\, d^2}{16\sqrt{3}}. \tag{6}$$

We developed a method for finding the optimal value of α which is described in section 3. In Fig. 1 we show the 2D and 3D contour maps of JFPM with $p = 7,\ p = 8\,,\ p = 9$.

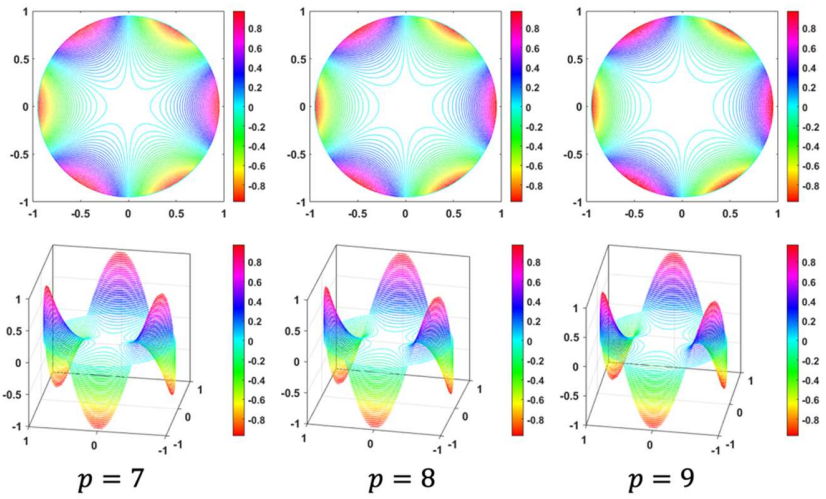

Fig. 1: Contour maps for phase masks in 2D and 3D.

3.- Phase mask thickness optimization

To determine the optimal thickness Δt of each phase mask we used the Average Difference (AD)[24] metric given by Eq. 7:

$$AD = \sum_{j=1}^{M} \sum_{i=1}^{N} [I_{6m} - I_{1m}]/MN, \tag{7}$$

where I_{6m} and I_{1m} are the image obtained for the optotype distance of 6 m and 1 m respectively. The pupil diameter is of 4 mm, N and M are the dimensions of the image of the optotype. The equation is evaluated at each of the wavelengths. The optimum value is achieved when:

$$AD_r - AD_b = 0, \tag{8}$$

Finally, the merit function is defined as the point where the AD of the images generated with the red and blue wavelength (channels red and blue of the RGB image respectively) are equal with respect to the image generated with the green wavelength (channel green of the RGB image). The values obtained for Δt are 13 μm for p = 7, 22 μm for p = 8, and 38 μm for the p = 9 case; in the case of highly transparent thermoplastic polymer material, methyl methacrylate (PMMA). With $n_C = 1.4879$, $n_d = 1.4906$, and $n_F = 1.4971$, where n_C , n_d, and n_F are the refractive indices of the PMMA for the wavelengths of the Fraunhofer C, d, and F spectral lines.

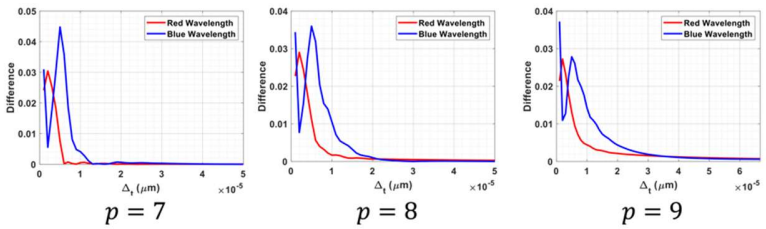

Fig. 2: Average Difference.

4.- Optical metrics

We characterized the performance of the different JFPM using two criteria. Firs, to analyze the involvement of NTF in the improvement of retinal images within the method, a new metric is used, it is called the MTF system defined in eq. 9 as:

$$MTF_{sys} = MTF \cdot NTF, \tag{9}$$

and the VScombined proposed by Young et al.[19] defined in eq. 10, which combines the OTF and the PTF in the calculation of the Visual Strehl criterion, emphasizing the weight of the phase of the OTF on the Visual Strehl calculation.

$$\boldsymbol{VS_{Combined}} = \frac{\int_{-\infty}^{\infty}\int_{-\infty}^{\infty} \boldsymbol{MTF(f_x,f_y)}\cdot\left|\boldsymbol{1-\frac{PTF(f_x,f_y)}{\pi}}\right|\boldsymbol{NTF(f_x,f_y)df_xdf_y}}{\int_{-\infty}^{\infty}\int_{-\infty}^{\infty} \boldsymbol{MTF(f_x,f_y)\cdot NTF(f_x,f_y)df_xdf_y}}, \tag{10}$$

where PTF is the Phase Transfer Function. We also used the simulates images for evaluating the performance of the JFPM. As objective criterion we have used the profile of the simulated retinal images of the optotypes. These profiles provide an idea of the contrast of the images. As subjective criterion, we used the retinal images provided by the simulations. These images allow the subjective quantification of the quality of the images.

6.- Results and Discussion

The Fig. 3 shows the MTF_{sys} corresponding to the different JFPM built with the optimum values of Δt. In all these cases the optotype is at 1 m. We also show the dependence with the pupil diameter. We have plotted the Neural Contrast Threshold[25, 26] (NCT) to show the intersection point with the MTF_{sys} to get an idea of the cutoff frequency of the system. The optotype has a AV of 0.1 LogMar, that corresponds to the frequency of the around of the 23.3 cyc/deg. The MTF_{sys} value is above the NCT contrast threshold in all cases for the frequency of the optotype (black line). This tells us that the retinal image is perceptible.

Fig. 4a shows the images obtained with the optotype of 0.1 LogMar, for the different pupil sizes, for the naked eye case (without including the JFPM). For the case of the object distance of $s_o = 6\,m$, it is possible to read the lines of "E" letter. However, in the case where the optotype is at $s_o = 1\,m$ the images quality is highly dependent on the pupil size. Other problem readily appreciated is the chromatic aberration due to the dispersion of the eye optics.

Figs. 4b, 4c, and 4d show the simulated images obtained with the optotype placed at $s_o = 1\,m$ and $s_o = 6\,m$, for the three different pupil diameters, 2 mm, 4 mm, and 6 mm, and for the JFPM p = 7, p =8, and p = 9 respectively. For p = 7 case, we can observe some artifacts ruining the image quality. These artifacts are more visible in the case of 2 mm diameter. We also appreciate a dependence of contrast with the pupil diameter, diminishing as the pupil increases.

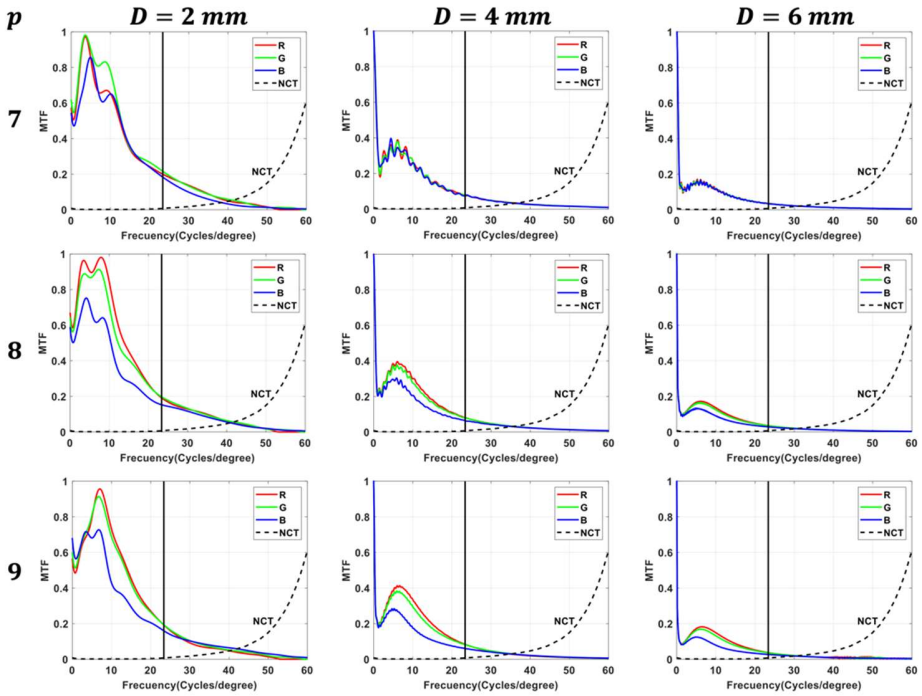

Fig. 3: MTF_{sys} with pupil size of 2 mm, 4 mm y 6 mm for $s_o = 1\ m$

With p = 8, these artifacts are less pronounced, and the contrast is higher than with p = 7. With p = 9, the artifacts are less than p = 8 and p = 7 cases, besides, the images show greater contrast than p = 7 and p = 8.

In addition, the decrease in the influence of chromatic aberration on the images is also evident. In general, there is a loss of contrast, more significant for cases where the pupil diameter is large. The method shows invariance to the pupil diameter in terms of the image shape but not at the contrast.

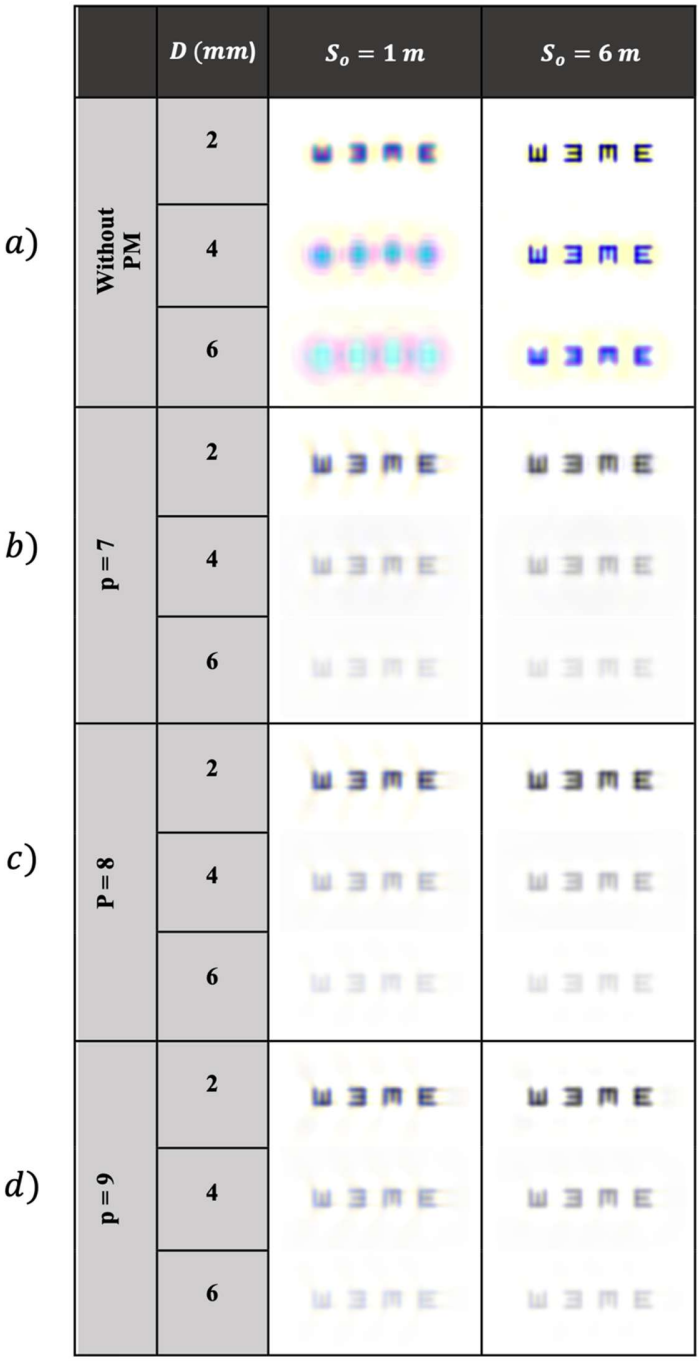

Fig. 4: Results for: a) without phase mask, b) with p=7, c) with p=8 and d) with p=9.

Fig. 5 shows the profiles of the images obtained of the optotypes. The best contrast is obtained with JFPM p = 9. It is noticeable that the profiles are nearly the same, presenting differences just in the contrast.

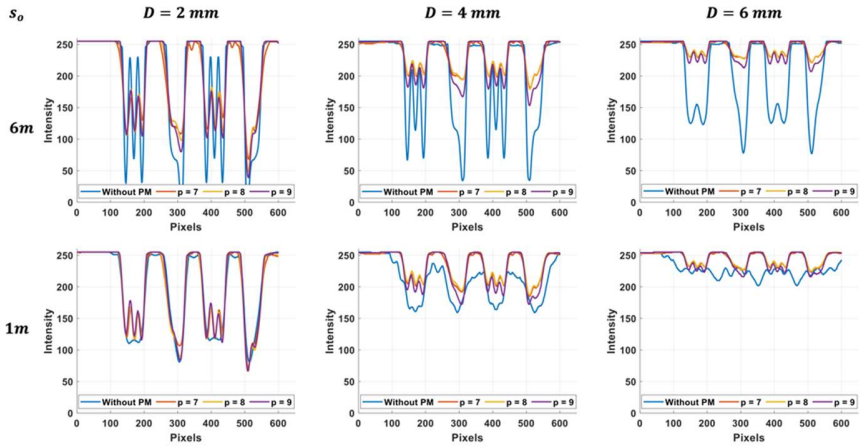

Fig. 5: Row profile for optotype with different pupil sizes and phase mask.

Fig. 6 shows the comparison of the profiles of the images obtained with each of the JFPM with the different pupil diameters. Again, we observe that the shape of the profiles are very stable, showing a decrease of the contrast as the diameter increases.

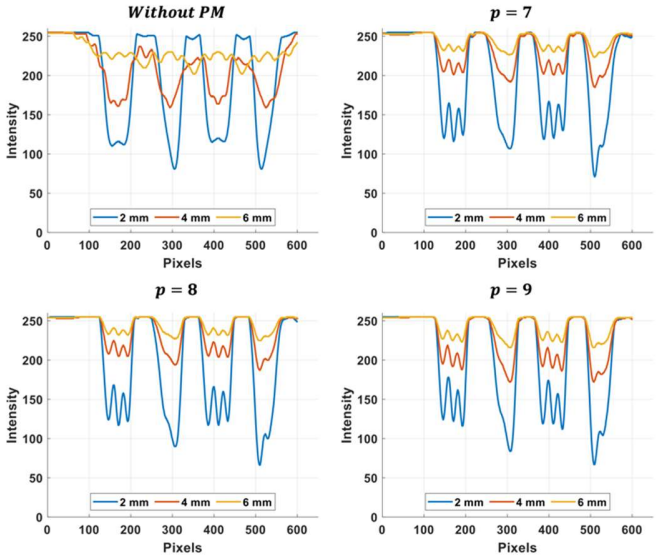

Fig. 6: Row profile for optotype comparison with different pupil sizes and phase masks for $S_o = 1\ m$.

Finally in Fig. 7 we show the results of the Visual Strehl criteria for the naked eye, and the eye with the different JFPM respectively.

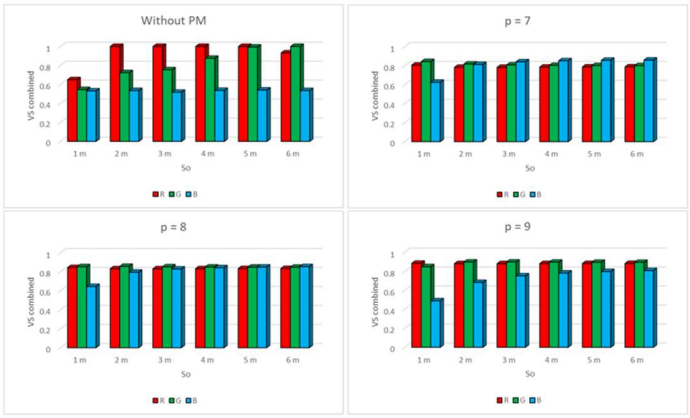

Figure 7: Metric VScombined for each case.

7.- Conclusions

1. The invariance of the PSF provided by the phase mask, in combination with the neuronal transfer function, allows us to observe objects with an AV of 0.1 LogMar units, in average values of the human visual system, with a pupil size of 2 mm, 4 mm, and 6 mm, but reducing the contrast of the final image.
2. We proposed the definition of the MTF of the system (MTFsys) which takes into account the Neural Transfer Function providing a more adequate description of the system.
3. The contrast of the final images after passing through the neural transfer filter is not only a function of the frequency but is also affected by the pupil size; at larger pupil sizes, the contrast decreases.
4. The use of Jacobi-Fourier phase masks as ophthalmic elements for presbyopia show promising results, with good range of clear vision, reduced pupil dependence and chromatic aberration.
5. The optimal parameter of the thickness of the phase mask delivers acceptable results regarding contrast and invariance. For the $p = 7$ the optimal $\Delta t = 13\,\mu m$, $\Delta t = 22\,\mu m$ for $p = 8$, and $\Delta t = 38\,\mu m$ for $p = 9$, according to the metric used to find the optimal parameter.
6. The Jacobi Fourier polynomials obtained with p=8 and p=9 provide similar results to that provided by trefoil Zernike phase mask, but with increased contrast and reduced amount of artifacts, contributing to a better identification of the optotypes.

Disclosures

The authors have no relevant financial interests in this article and no potential conflicts of interest to disclose. The other authors have no conflicts of interest to declare.

Code, Data, and Materials Availability

All data in support of the findings of this paper are available within the article.

Acknowledgments

Angel Salas Sánchez thanks to Consejo Nacional de Humanidades Ciencia y Tecnología (CONAHCYT); with CVU no. 1143898. This work was supported by Ministerio de Ciencia e Innovación and FEDER, grant No. PID2020-115909RB-I00, and Xunta de Galicia, grant No. ED431B 2023/07.

References

[1] Wolffsohn, J.S., & Davies, L.N., Presbyopia: Effectiveness of correction strategies, Progress in Retinal and Eye Research. (2018).

[2] Charman, W. N., "Developments in the correction of presbyopia I: spectacle and contact lenses," Ophthalmic Physiol. Opt. 34, 8-29 (2014).

[3] Charman, W. N., "Developments in the correction of presbyopia II: surgical approaches," Ophthalmic Physiol. Opt. 34, 397-426 (2014).

[4] Bennett, E. S., Jurkus, J. M., & Schwartz C. A. (2000), Clinical Manual of Contact Lenses, 2nd ed., pp. 410–449, Lippincott Williams & Wilkins, Philadelphia.

[5] Simonov, A. N., Vdovin, G. & Rombach, M., "Cubic optical elements for an accommodative intraocular lens," Opt. Exp. 14(17), 7757–7775 (2006).

[6] Mira-Agudelo, A., Torres-Sepúlveda, W., Barrera, J. F., Henao, R., Blocki, N., Petelczyc, K., & Kolodziejczyk, A. (2016). Compensation of presbyopia with the light sword lens. Investigative Ophthalmology & Visual Science, 57(15), 6870–6877.

[7] Galinier, Laurent & Renaud-Goud, Philippe & Brusau, Jean & Kergadallan, Lucien & Augereau, Jean & Simon, Bertrand. (2024). Spiral Diopter: Freeform Lenses With Enhanced Multifocal Behavior. Optica. 11. 10.1364/OPTICA.507066.

[8] Cathey Jr., W.T., "Extended depth of field optics for human vision," U.S. Patent 7025454B2 (2006).

[9] Zalevsky, Z., Yaish, S. B., Yehezkel, O., & Belkin, M., "Thin spectacles for myopia, presbyopia and astigmatism insensitive vision," Opt. Exp. 15(17), 10790–10803 (2007).

[10] Gallego, A. A., Bará, S., Jaroszewicz, Z., & Kolodziejczyk, A., "Visual Strehl performance of IOL designs with extended depth of focus," Optom. Vision Sci. 89(12), 1702-1707 (2012).

[11] Petelczyc, K., Bará, S., López, A. C., Jaroszewicz, Z., Kakarenko, K., & Kolodziejczyk, A., "Contrast transfer characteristics of the light sword optical element designed for presbyopia compensations," J. Eur. Opt. Soc. Rapid Publ. 6, 11053 (2011).

[12] Arines, J., Almaguer, C., & Acosta, E., "Potential use of cubic phase masks for extending the range of clear vision in presbyopes: initial calculation and simulation studies," Ophthalmic Physiol. Opt., 37(2), 141-150 (2017).

[13] González-Amador, E., Padilla-Vivanco, A., Toxqui-Quitl, C., Arines, J., & Acosta, E., "Jacobi–Fourier phase mask for wavefront coding," Optics and Lasers in Engineering, 126, 105880 (2020).

[14] Acosta, E. Olvera-Angeles, M. González-Amador, E. Sasian, J. Schwiegerling, J., & Arines, J., "Wavefront coding with Jacobi–Fourier phase masks for retinal imaging. Applied Optics, G234-G238 (2020).

[15] Dowski E. R., & Cathey W. T., Extended depth of field through wave-front coding. Applied Optics, 1859-1866 (1995).

[16] Watson, A. B., & Ahumada, A. J., "A standard model for foveal detection of spatial contrast," J. Vision 5, 717–740 (2005).
[17] Watson, A. B., & Ahumada, A. J., "Modeling acuity for optotypes varying in complexity," J. Vision 12(10), 19–19 (2012).
[18] Marsack, J. D., Thibos, L. N. & Applegate, R. A., Metrics of optical quality derived from wave aberrations predict visual performance. J. Vision, 4-4 (2004).
[19] Young, L. K., Love, G. D., & Smithson, H. E., "Accounting for the phase, spatial frequency and orientation demands of the task improves metrics based on the visual Strehl ratio," Vision Res. 90, 57–67 (2013).
[20] Young, L. K., Love, G. D., & Smithson, H. E., "Different aberrations raise contrast thresholds for single-letter identification in line with their effect on cross-correlation based confusability," J. Vision 13(7), 12–12 (2013).
[21] Atchison, D. A & Thibos, L. N., "Optical models of the human eye," Clinical and experimental optometric 99(2), 99-106 (2016).
[22] Malacara D. (2015), Óptica básica, Ediciones científicas universitarias 3a edición.
[23] Thibos, L. N., Ye, M., Zhang, X., & Bradley, A., "The chromatic eye: a new reduced-eye model of ocular chromatic aberration in humans." Applied Optics 31(19), 3594-3600 (1992).
[24] Eskicioglu, A. M., & Fisher, P. S., "Image quality measures and their performance," IEEE Transactions on communications 43(12), 2959-2965 (1995).
[25] Rabbetts R. B., (2007), Clinical Visual Optics, Editorial BUTTERWORTH, 2a edition.
[26] McAnany, J. J., Alexander, K. R., Lim, J. I. & Shahidi, M., "Object frequency characteristics of visual acuity," Investigative Ophthalmology & Visual Science 52(13), 9534-9538 (2011).